Mol. Cells *32*, 431-435, November 30, 2011
DOI/10.1007/s10059-011-0102-y

Molecules and Cells

Crystal Structure of Phosphopantetheine Adenylyltransferase from *Enterococcus faecalis* in the Ligand-Unbound State and in Complex with ATP and Pantetheine

Hye-Jin Yoon[1], Ji Yong Kang[1], Bunzo Mikami[2], Hyung Ho Lee[3,4,*], and Se Won Suh[1,5,*]

Phosphopantetheine adenylyltransferase (PPAT) catalyzes the reversible transfer of an adenylyl group from ATP to 4′-phosphopantetheine (Ppant) to form dephospho-CoA (dPCoA) and pyrophosphate in the Coenzyme A (CoA) biosynthetic pathway. Importantly, PPATs are the potential target for developing antibiotics because bacterial and mammalian PPATs share little sequence homology. Previous structural studies revealed the mechanism of the recognizing substrates and products. The binding modes of ATP, ADP, Ppant, and dPCoA are highly similar in all known structures, whereas the binding modes of CoA or 3′-phosphoadenosine 5′-phosphosulfate binding are novel. To provide further structural information on ligand binding by PPATs, the crystal structure of PPAT from *Enterococcus faecalis* was solved in three forms: (i) apo form, (ii) binary complex with ATP, and (iii) binary complex with pantetheine. The substrate analog, pantetheine, binds to the active site in a similar manner to Ppant. The new structural information reported in this study including pantetheine as a potent inhibitor of PPAT will supplement the existing structural data and should be useful for structure-based antibacterial discovery against PPATs.

INTRODUCTION

Coenzyme A (CoA) is required in several key reactions in the intermediary metabolism as an essential cofactor (Geerlof et al., 1999; Lee et al., 2004; Leonardi et al., 2005). In bacteria, it is synthesized in five steps from pantothenate (vitamin B5), cysteine, and ATP (Robishaw et al., 1985). The penultimate step in this biosynthetic pathway is catalyzed by phosphopante-theine adenylyl-transferase (PPAT), a member of the nucleotidyltransferase super-family (Bork et al., 1995). This enzyme catalyzes the reversible transfer of an adenylyl group from ATP to 4′-phosphopantethe-ine (Ppant), yielding dephospho-CoA (dPCoA) and pyrophosphate (Izard and Geerlof, 1999). In contrast to bacteria, PPAT and dephospho-CoA kinase occur as a bifunctional enzyme known as CoA synthase in mammals (Aghajanian and Worrall, 2002). Bacterial PPATs and mammalian PPATs are highly dissimilar in their primary sequences, making the bacterial PPATs an attractive target for antibacterial discovery (Miller et al., 2010). Based on the inhibitor-bound structure of *Escherichia coli* PPAT, a potent and specific inhibitor with an IC_{50} of 6 nM against *E. coli* PPAT but no activity against porcine PPAT, was discovered (Zhao et al., 2003).

The crystal structures of *E. coli* PPAT in complex with dPCoA (Izard and Geerlof, 1999), ATP (Izard, 2002), Ppant (Izard, 2002), and CoA (Izard, 2003) have been reported. *E. coli* PPAT is a homohexamer with 32 point group symmetry. Ppant (Izard, 2002) and dPCoA (Izard and Geerlof, 1999) are bound to only one trimeric unit within the hexamer of *E. coli* PPAT, whereas ATP is bound to both trimeric units of the hexamer (Izard, 2002). In the crystal structure of *E. coli* PPAT bound with CoA, a feedback regulator, the adenylyl moiety of CoA was bound to a site that did not overlap with the binding site of dPCoA, the product (Izard, 2003). The crystal structure of *Staphylococcus aureus* PPAT in complex with 3′-phos-phoadenosine 5′-phosphosulfate was recently reported, which revealed a new mode of ligand binding to PPAT (Lee et al., 2009). The structures of *Mycobacterium tuberculosis* PPAT in the apo form (Morris and Izard, 2004), *Thermus thermophilus* PPAT in complex with Ppant (Takahashi et al., 2004), and *Ba-cillus subtilis* PPAT in complex with ADP (Badger et al., 2005) were also reported. Furthermore, the structures of an archaeal PPAT (Protein Data Bank ID code 3do8; unpublished) and a mammalian bifunctional coenzyme A synthase covering the C-terminal one third of PPAT and the entire dephospho-CoA kinase (PDB ID code 2f6r; Joint Center for Structural Genomics, unpublished) were solved. Recently, the crystal structures of *M. tuberculosis* PPAT in complex with Ppant and the nonhydrolyz-able ATP analogue [(α, β)-methyleno]triphosphate were re ported (Wubben and

[1]Department of Chemistry, College of Natural Sciences, Seoul National University, Seoul 151-742, Korea, [2]Laboratory of Quality Design and Exploitation, Division of Agronomy and Horticultural Science, Graduate School of Agriculture, Kyoto University, Kyoto 611-0011, Japan, [3]Department of Bio and Nano Chemistry, Kookmin University, Seoul 136-702, Korea, [4]Department of Integrative Biomedical Science and Engineering, Kookmin University, Seoul 136-702, Korea, [5]Department of Biophysics and Chemical Biology, College of Natural Sciences, Seoul National University, Seoul 151-742, Korea
*Correspondence: sewonsuh@snu.ac.kr (SWS); hhlee@kookmin.ac.kr (HHL)

Received May 11, 2011; revised August 21, 2011; accepted August 23, 2011; published online September 9, 2011

Keywords: coenzyme A biosynthetic pathway, *Enterococcus faecalis*, pantetheine, phosphopantetheine adenylyltransferase, PPAT

Mesecar, 2010).

The use of vancomycin has continued to expand due to the increasing number of patients infected or colonized with methicillin-resistant *S. aureus*, causing an increase in the prevalence of vancomycin-resistant *Enterococcus* (Mazuski, 2008). The resistance in enterococci is a major threat for genetic transfer and the emergence of increasing numbers of vancomycin-resistant *S. aureus* (Mazuski, 2008). *Enterococcus faecalis* is a Gram-positive pathogen that causes many of the same problems as other members of the intestinal flora, which include opportunistic urinary tract infections and wound infections. It can cause life-threatening infections in humans, particularly in a nosocomial environment. To aid in the structure-based discovery of new antibacterial compounds against major human pathogens including *E. faecalis*, detailed structural information on the binding modes of different ligands to the PPAT active site would be useful. In this study, the crystal structure of *E. faecalis* PPAT was determined in three forms, i.e. in the apo form and as binary complexes with ATP or pantetheine, to provide further structural information on ligand binding by PPATs. Until now, no structure of any PPAT in complex with pantetheine has been reported.

MATERIALS AND METHODS

Protein expression, purification, and crystallization

The overexpression of the recombinant *E. faecalis* PPAT with a C-terminal His_6-containing tag was previously reported (Kang et al., 2006). In this study, its new crystal form was obtained in the orthorhombic space group, which is different from the previously reported crystal in the tetragonal space group (Kang et al., 2006). The new crystal form is more suitable for a high resolution structure determination than the previous tetragonal crystal form (Kang et al., 2006). The new crystals of the apo enzyme were grown at 24°C by mixing equal volumes (2 μl each) of the protein solution (20 mg ml^{-1} concentration in 20 mM Tris-HCl, pH 7.5, and 200 mM NaCl) and the reservoir solution consisting of 3.5 M sodium formate and 100 mM Tris-HCl (pH 8.5). The apo crystals grew to approximate dimensions of 0.1 mm × 0.1 mm × 0.1 mm within a few days. Crystals of the ATP- or pantetheine-bound enzyme were grown by soaking the apo crystals in a reservoir solution containing 50 mM ATP (or pantetheine) for 5 min before cryo protection.

Structure determination and refinement

The crystals were frozen using a cryoprotectant solution containing 25% (*v/v*) glycerol in the crystallization mother liquor. X-ray diffraction data of the apo form and the ATP-complex were collected at 100 K on an Area Detector Systems Corporation Quantum 4R CCD detector at the experimental station BL-17A of the Photon Factory, Japan. Data of the pantetheine-bound crystal were collected at 100 K on an Area Detector Systems Corporation Quantum 315 CCD detector at the experimental station BL-5A of the Photon Factory, Japan. For each image, the crystal was rotated by 1°. The raw data were processed and scaled using the *HKL*-2000 program suite (Otwinowski and Minor, 1997). Table 1 summarizes the statistics of data collection. The apo-form crystal belongs to the space group $P2_12_12_1$, with unit cell parameters of a = 110.20 Å, b = 125.68 Å, and c = 125.82 Å (Table 1). Six monomers are present in the asymmetric unit, giving a crystal volume per protein mass (V_M) of 3.68 $Å^3$ Da^{-1} and a solvent content of 67%, respectively.

The apo structure of *E. faecalis* PPAT was solved by the molecular replacement method using the hexamer model of *T. maritima* PPAT (PDB ID: 1vlh; Joint Center for Structural Genomics, unpublished). A cross-rotational search followed by a translational search was performed using the *CNS* program (Brünger, 2007; Brünger et al., 1998). Subsequent manual model building was carried out using the *O* program (Jones et al., 1991). The model was refined by minimizing the maximum-likelihood target function on amplitudes using the *CNS* program (Brünger, 2007; Brünger et al., 1998), including the bulk solvent correction. Several rounds of model building, simulated annealing, positional refinement, and individual *B*-factor refinement were performed. This apo model was used to refine the ATP- and pantetheine-bound structures. The stereochemistry of the refined models was evaluated using the *MolProbity* program (Davis et al., 2007). Table 1 lists the refinement statistics.

RESULTS AND DISCUSSION

Model quality and structural comparisons

The structure of *E. faecalis* PPAT in three forms was determined: (i) the apo form at 2.3 Å resolution, (ii) a binary complex with ATP at 2.3 Å resolution, and (iii) a binary complex with pantetheine at 2.4 Å resolution. The refined models gave R_{work}/R_{free} values of 19.6/24.9% for 20-2.30 Å, 20.6/24.5% for 20-2.30 Å, and 21.3/26.2% for 20-2.40 Å data, respectively, for the apo, ATP-bound, and pantetheine-bound forms (Table 1). The refined models of the apo, ATP-bound, and pantetheine-bound PPAT account for residues 1-38 and 45-158 in each of the six monomers in an asymmetric unit. The C-terminal residues (Lys159-Ser163) and C-terminal fusion tag (LEHHHHHH) of the recombinant enzyme are disordered in all six monomers of the three models. All the non-glycine residues are in the most favored and allowed regions of the Ramachandran plot for the three models (Table 1).

Six monomers of *E. faecalis* PPAT in the asymmetric unit are almost identical to each other. When monomer A was compared with the other monomers, the r.m.s. deviations averaged over the five monomers B-F were 0.7 Å, 0.7 Å, and 0.8 Å for 158 Cα atom pairs for the apo, ATP-bound, and pantetheine-bound structures, respectively. When monomer A of the apo model was overlapped with monomer A of the ATP- and pantetheine-complex models, the r.m.s. deviations were 0.48 Å and 0.40 Å for 152 Cα atoms, respectively. When monomer A of the ATP-complex model was compared with monomer A of the pantetheine-complex model, the r.m.s. deviation was 0.63 Å for 152 Cα atoms. This suggests that all three structures of *E. faecalis* PPAT are similar to each other. When six monomers of the apo model were overlapped with those of the ATP- and pantetheine-complex models, the r.m.s. deviations were 0.72 Å and 0.47 Å for 912 Cα atoms, respectively. The r.m.s. deviation was 0.81 Å for 912 Cα atoms when six monomers of the ATP-complex model were compared with those of the pantetheine-complex model. This indicates that there is no significant change in the oligomeric structure of *E. faecalis* PPAT upon ligand binding.

Overall monomer and hexamer structures

A monomer of *E. faecalis* PPAT adopts the dinucleotide-binding fold (or the canonical Rossmann fold) (Rossmann et al., 1975). The core contains a five-stranded parallel β-sheet, arranged in the order, β3-β2-β1-β4-β5, which is packed on one side by five α-helices (α1, α2, α5, α6, and α7) and on the other side by two α-helices (α3 and α4) (Fig. 1A). *E. faecalis* PPAT is hexameric and displays 32 symmetry (Fig. 1B). In the ligand-bound structures of *E. faecalis* PPAT, all six subunits are bound with the ligand (Fig. 1B). This is similar to *T. thermophilus* PPAT in complex with Ppant (Takahashi et al., 2004), *B. sub-*

Table 1. Statistics for data collection and refinement

Data set	Apo	ATP	Pantetheine
A. Data collection statistics			
X-ray source	PF BL-17A	PF BL-17A	PF BL-5A
X-ray wavelength (Å)	1.00000	1.00000	1.00000
Space group	$P2_12_12_1$	$P2_12_12_1$	$P2_12_12_1$
a (Å)	110.20	112.79	109.64
b (Å)	125.68	123.91	125.79
c (Å)	125.82	124.23	125.80
Resolution range (Å)	20-2.30	20-2.30	20-2.40
Total / unique reflections	366,306/76,265	534,418/76,960	438,106/68,248
Completeness (%)	98.3 (98.5)[a]	98.9 (97.9)[a]	99.5 (96.4)[a]
Average $I/\sigma(I)$	14.1 (4.1)[a]	17.7 (10.9)[a]	10.3 (3.7)[a]
R_{merge}[b] (%)	8.3 (38.3)[a]	6.5 (23.2)[a]	9.4 (37.2)[a]
B. Model refinement statistics			
R_{work} / R_{free}[c] (%)	19.6/24.9	20.6/24.5	21.3/26.2
Number / average *B*-factor (Å^2)			
Protein nonhydrogen atoms atoms	6 × 1,226/42.8	6 × 1,226/44.2	6 × 1,226/47.8
Water oxygen atoms	534/43.5	416/41.9	254/42.4
Ligand molecules	None	6 × ATP / 40.7	6 × pantetheine / 56.5
R.m.s. deviations from ideal geometry			
Bond lengths (Å)	0.007	0.008	0.007
Bond angles (°)	1.23	1.19	1.04
MolProbity protein-geometry analysis			
Ramachandran favored (%)	97.1 (862/888)	96.4 (856/888)	97.5 (866/888)
Ramachandran allowed (%)	2.9 (26/888)	3.6 (32/888)	2.5 (22/888)
Ramachandran outliers (%)	0.0 (0/888)	0.0 (0/888)	0.0 (0/888)
MolProbity score	2.58	2.68	2.67

[a]Values in parentheses refer to the highest resolution shell (apo, 2.38-2.30 Å; ATP, 2.38-2.30 Å; pantetheine, 2.49-2.40 Å, respectively).
[b]$R_{merge} = \Sigma_{hkl}\Sigma_i | I_i(hkl) - \langle I(hkl)\rangle | / \Sigma_{hkl}\Sigma_i I_i(hkl)_i$, where $I(hkl)$ is the intensity of reflection *hkl*, Σ_{hkl} is the sum over all reflections, and Σ_i is the sum over i measurements of reflection *hkl*.
[c]$R = \Sigma_{hkl} | |F_{obs}| - |F_{calc}| | / \Sigma_{hkl} |F_{obs}|$, where R_{free} was calculated for a randomly chosen 10% of reflections, which were not used for structure refinement and R_{work} was calculated for the remaining.

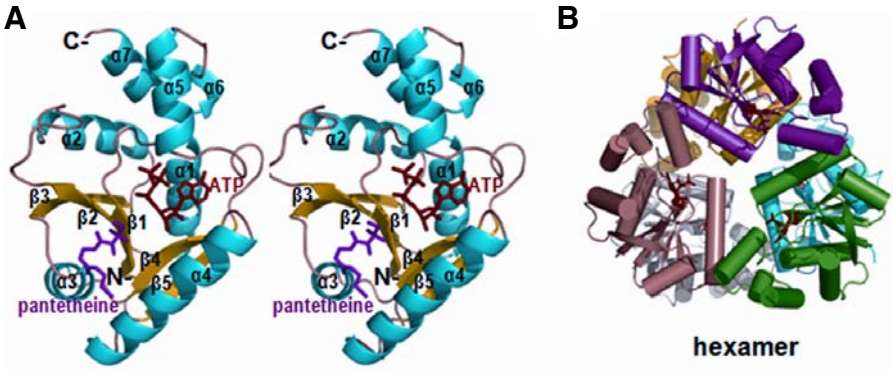

Fig. 1. Monomer and hexamer structures of *E. faecalis* PPAT. (A) Stereo ribbon diagram of the monomer (apo) in stereo. The α-helices, β-strands, and loops are colored in cyan or yellow, and pink, respectively. This composite figure was produced by incorporating ATP and pantetheine into the apo structure. ATP and pantetheine (colored in red and magenta, respectively) bound in the active site are shown in stick models. (B) Ribbon diagram of the hexamer (ATP complex). ATP (colored in red) bound in the active site is shown as a stick model.

tilis PPAT in complex with ADP (Badger et al., 2005), and *S. aureus* PPAT in complex with 3′-phosphoadenosine 5′-phosphosulfate (Lee et al., 2009). In contrast, *E. coli* PPAT is bound to either Ppant or dPCoA in only one of the two trimeric units (Izard, 2002; Izard and Geerlof, 1999). The overall monomer and hexamer structures of *E. faecalis* PPAT are similar to those of the other bacterial PPATs (Badger et al., 2005; Izard, 2002; 2003; Izard and Geerlof, 1999; Lee et al., 2009; Morris and Izard, 2004; Takahashi et al., 2004) (Fig. 2).

Binding modes of ATP and pantetheine

In the ligand-complexed structures of *E. faecalis* PPAT, ATP or

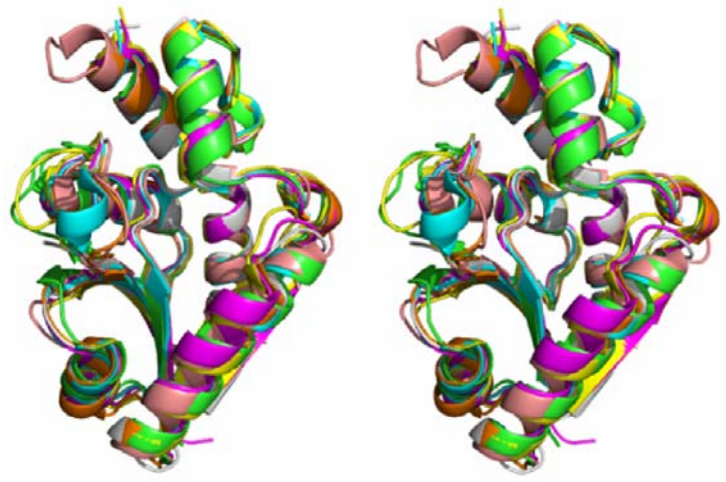

Fig. 2. Structural comparison of PPATs. Superposition of *E. faecalis* PPAT (PDB ID code 3ND5, colored in green) with PPATs from *E. coli* (PDB ID code 1QJC, colored in cyan), *M. tuberculosis* (PDB ID code 1TFU, colored in yellow), *S. aureus* (PDB ID code 3F3M, colored in magenta), *T. thermophilus* (PDB ID code 1OD6, colored in grey), *B. subtilis* (PDB ID code 1O6B, colored in pink), and *T. maritima* (PDB ID code 1VLH, colored in orange).

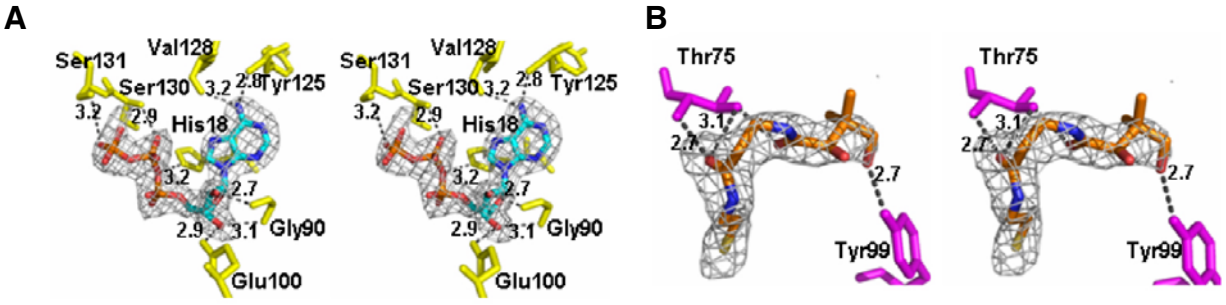

Fig. 3. Stereo view of the *Fo* - *Fc* OMIT electron density map of (A) ATP (chain A) and (B) pantetheine (chain F) contoured at the 3.0 and 2.5 sigma level, respectively. With 100% occupancy, the mean *B*-factor (56.5 Å^2) of pantetheine is slightly higher than that of the protein atoms (47.8 Å^2). In particualr, the mean *B*-factor of 6 pantetheines from chain A to F were 63.7, 57.2, 54.5, 50.3, 55.1, and 43.4 Å^2. Black dotted lines denote hydrogen bonds (Å).

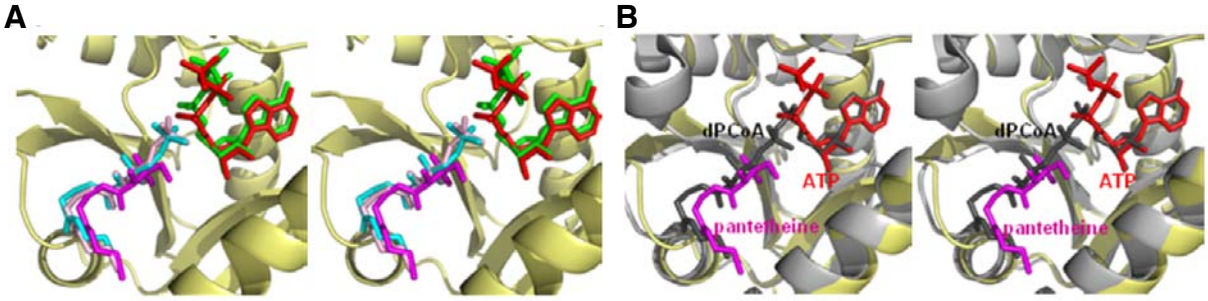

Fig. 4. Stereo view of the active site of *E. faecalis* PPAT. (A) Ribbon diagram of the active site around ATP and pantetheine bound to *E. faecalis* PPAT. This composite figure was produced by incorporating pantetheine (colored in magenta) of *E. faecalis* PPAT, ATP (colored in green, 1GN8) and Ppant (colored in cyan, 1QJC) of *E. coli* PPAT, and Ppant (colored in pink, 1OD6) of *T. thermophilus* PPAT into the ATP complex structure of *E. faecalis* PPAT (colored in red). ATP, pantetheine, and Ppant bound in the active site are shown in stick models. (B) Ribbon diagram of the active site around ATP and pantetheine bound to *E. faecalis* PPAT, and dPCoA bound to *E. coli* PPAT (1B6T). This composite figure was produced by incorporating pantetheine and dPCoA into the ATP complex structure of *E. faecalis* PPAT. ATP (colored in red), pantetheine (colored in magenta), and dPCoA (colored in gray) bound in the active site are shown in the stick models. All figures were produced using *PyMOL* (http://www.pymol.org).

pantetheine is clearly defined by the electron density and is bound in the active site of all six chains of the homohexamer (Fig. 3). In the ATP-bound structure (chain A) of *E. faecalis* PPAT, His18 (nitrogen atom), Gly90 (oxygen and nitrogen atoms), Glu100 (oxygen atom), Tyr125 (oxygen atom), Val128 (oxygen atom), Ser130 (nitrogen atom), and Ser131 (oxygen atom) make 8 hydrogen bonds with oxygen or nitrogen atoms of ATP (Fig. 3A). The binding mode of ATP in the *E. faecalis* PPAT structure is highly similar to that in the ATP-bound structure of *E. coli* PPAT (Izard, 2002), despite the absence of the

electron density of a catalytic metal ion (Mn^{2+}) around the phosphates of ATP in *E. faecalis* PPAT (Fig. 4A). The substrate analog, pantetheine, is bound to *E. faecalis* PPAT in a similar manner to that in the Ppant complex structures of *E. coli* PPAT (PDB ID: 1QJC, Izard, 2002), *T. thermophilus* PPAT (1OD6; Takahashi et al., 2004), and *T. maritima* PPAT (1VLH; Joint Center for Structural Genomics, unpublished) (Fig. 4B). In the pantetheine-bound structure of *E. faecalis* PPAT, Tyr99 (oxygen atom) and Thr75 (oxygen and nitrogen atoms) make one and three hydrogen bonds with oxygen atoms of pantetheine, respectively (Fig. 3B). The same oxygen atoms (make hydrogen bonds with Thr75 in *E. faecalis* PPAT) of Ppant make van der Waals interactions with the side chains of Met74 in *E. coli* PPAT, Leu74 in *T. thermophilus* PPAT, and Leu72 in *T. maritima* PPAT. Overall, pantetheine has a similar conformation to Ppant and binds to the active site in a similar manner to Ppant even though pantetheine lacks the phosphate group attached to the pantetheine moiety. This study provides additional structural information on ligand binding by *E. faecalis* PPAT for the structure-based design of PPAT inhibitors mimicking Ppant as a potential antibacterial agent.

ACKNOWLEDGMENTS

The authors wish to thank the beamline staffs for their assistance during data collection (BL-5A and BL-17A of Photon Factory, Japan). This work was supported by the Korea Ministry of Education, Science, and Technology, National Research Foundation of Korea through the Basic Science Outstanding Scholars Program, World-Class University Program (Grant no. 305-20080089) and the Korea Ministry for Health, Welfare & Family Affairs (Korea Healthcare Technology R&D Project, Grant no. A092006) to SWS and by Seoul R&BD Program (ST100072) to HHL. This research was also supported by the Basic Science Research Program through the National Research Foundation of Korea funded by the Ministry of Education, Science and Technology (2010-0005805) to HHL and (2011-0013663) to HJY. This work was also supported by the research program 2011 of Kookmin University to HHL.

REFERENCES

Aghajanian, S., and Worrall, D.M. (2002). Identification and characterization of the gene encoding the human phosphopantetheine adenylyltransferase and dephospho-CoA kinase bifunctional enzyme (CoA synthase). Biochem. J. *365*, 13-18.

Badger, J., Sauder, J.M., Adams, J.M., Antonysamy, S., Bain, K., Bergseid, M.G., Buchanan, S.G., Buchanan, M.D., Batiyenko, Y., Christopher, J.A., et al. (2005). Structural analysis of a set of proteins resulting from a bacterial genomics project. Proteins *60*, 787-796.

Bork, P., Holm, L., Koonin, E.V., and Sander, C. (1995). The cytidylyltransferase superfamily: identification of the nucleotide-binding site and fold prediction. Proteins *22*, 259-266.

Brünger, A.T. (2007). Version 1.2 of the crystallography and NMR system. Nat. Protoc. *2*, 2728-2733.

Brünger, A.T., Adams, P.D., Clore, G.M., DeLano, W.L., Gros, P., Grosse-Kunstleve, R.W., Jiang, J.S., Kuszewski, J., Nilges, M., Pannu, N.S., et al. (1998). Crystallography & NMR system: A new software suite for macromolecular structure determination. Acta Cryst. *D54*, 905-921.

Davis, I.W., Leaver-Fay, A., Chen, V.B., Block, J.N., Kapral, G.J., Wang, X., Murray, L.W., Arendall, W.B., 3rd, Snoeyink, J., Richardson, J.S., et al. (2007). MolProbity: all-atom contacts and structure validation for proteins and nucleic acids. Nucleic Acids Res. *35*, W375-W383.

Geerlof, A., Lewendon, A., and Shaw, W.V. (1999). Purification and characterization of phosphopantetheine adenylyltransferase from *Escherichia coli*. J. Biol. Chem. *274*, 27105-27111.

Izard, T. (2002). The crystal structures of phosphopantetheine adenylyltransferase with bound substrates reveal the enzyme's catalytic mechanism. J. Mol. Biol. *315*, 487-495.

Izard, T. (2003). A novel adenylate binding site confers phosphopantetheine adenylyltransferase interactions with coenzyme A. J. Bacteriol. *185*, 4074-4080.

Izard, T., and Geerlof, A. (1999). The crystal structure of a novel bacterial adenylyltransferase reveals half of sites reactivity. EMBO J. *18*, 2021-2030.

Jones, T.A., Zou, J.Y., Cowan, S.W., and Kjeldgaard, M. (1991). Improved methods for building protein models in electron density maps and the location of errors in these models. Acta Cryst. *A47*, 110-119.

Kang, J.Y., Lee, H.H., Yoon, H.J., Kim, H.S., and Suh, S.W. (2006). Overexpression, crystallization and preliminary X-ray crystallographic analysis of phosphopantetheine adenylyltransferase from *Enterococcus faecalis*. Acta Cryst. *F62*, 1131-1133.

Lee, S.S., Jeong, W.J., Bae, J.M., Bang, J.W., Liu, J.R., and Har, C.H. (2004). Characterization of the plastid-encoded carboxyltransferase subunit (accD) gene of potato. Mol. Cells *17*, 422-429.

Lee, H.H., Yoon, H.J., Kang, J.Y., Park, J.H., Kim, D.J., Choi, K.H., Lee, S.K., Song, J., Kim, H.J., and Suh, S.W. (2009). The structure of Staphylococcus aureus phosphopantetheine adenylyltransferase in complex with 3′-phosphoadenosine 5′-phosphosulfate reveals a new ligand-binding mode. Acta Crystallogr. Sect. F Struct. Biol. Cryst. Commun. *F65*, 987-991.

Leonardi, R., Zhang, Y.M., Rock, C.O., and Jackowski, S. (2005). Coenzyme A: back in action. Prog. Lipid Res. *44*, 125-153.

Mazuski, J.E. (2008). Vancomycin-resistant enterococcus: risk factors, surveillance, infections, and treatment. Surg. Infect. (Larchmt) *9*, 567-571.

Miller, J.R., Thanabal, V., Melnick, M.M., Lall, M., Donovan, C., Sarver, R.W., Lee, D.Y., Ohren, J., and Emerson, D. (2010). The use of biochemical and biophysical tools for triage of high-throughput screening hits - A case study with *Escherichia coli* phosphopantetheine adenylyltransferase. Chem. Biol. Drug Des. *75*, 444-454.

Morris, V.K., and Izard, T. (2004). Substrate-induced asymmetry and channel closure revealed by the apoenzyme structure of *Mycobacterium tuberculosis* phosphopantetheine adenylyltransferase. Protein Sci. *13*, 2547-2552.

Otwinowski, Z., and Minor, W. (1997). Processing of X-ray diffraction data collected in oscillation mode. Methods Enzymol. *276*, 307-326.

Robishaw, J.D., and Neely, J.R. (1985). Coenzyme A metabolism. Am. J. Physiol. *248*, E1-E9.

Rossmann, M.G., Liljas, A., Brändén, C.I., and Banaszak, L.J. (1975). Evolutionary and structural relationship among dehydrogenases. The Enzymes, *11*, 61-102.

Takahashi, H., Inagaki, E., Fujimoto, Y., Kuroishi, C., Nodake, Y., Nakamura, Y., Arisaka, F., Yutani, K., Kuramitsu, S., Yokoyama, S., et al. (2004). Structure and implications for the thermal stability of phosphopantetheine adenylyltransferase from *Thermus thermophilus*. Acta Crystallogr. D Biol. Crystallogr. *60(Pt 1)*, 97-104.

Wubben, T., and Mesecar, A.D. (2010). Kinetic, thermodynamic, and structural insight into the mechanism of phosphopantetheine adenylyltransferase from *Mycobacterium tuberculosis*. J. Mol. Biol. *404*, 202-219.

Zhao, L., Allanson, N.M., Thomson, S.P., Maclean, J.K., Barker, J.J., Primrose, W.U., Tyler, P.D., and Lewendon, A. (2003). Inhibitors of phosphopantetheine adenylyltransferase. Eur. J. Med. Chem. *38*, 345-349.